Journal of Medicinal Chemistry Article

J. Med. Chem. **2010,** *53,* 4009–4017 **4009**
DOI: 10.1021/jm901850k

Structure−Activity Relationships of Fluorinated (*E*)-3-((6-Methylpyridin-2-yl)ethynyl)cyclohex-2-enone-*O*-methyloxime (ABP688) Derivatives and the Discovery of a High Affinity Analogue as a Potential Candidate for Imaging Metabotropic Glutamate Recepors Subtype 5 (mGluR5) with Positron Emission Tomography (PET)

Cindy A. Baumann,[†] Linjing Mu,[†] Sinja Johannsen, Michael Honer, Pius A. Schubiger, and Simon M. Ametamey*

Center for Radiopharmaceutical Sciences of ETH, PSI and USZ, Department of Chemistry and Applied Biosciences of ETH Zurich, Switzerland, Wolfgang-Pauli Strasse 10, 8093 Zurich, Switzerland. [†]*Both authors contributed equally.*

Received December 15, 2009

The metabotropic glutamate receptor subtype 5 (mGluR5) is recognized to be involved in numerous brain disorders. In an effort to obtain a fluorine-18 labeled analogue of the mGluR5 PET tracer [^{11}C]ABP688, 13 novel ligands based on the core structure of ABP688 were synthesized. Molecules in which the methyl group at the oxime functionality of ABP688 was replaced by fluorobenzonitriles, fluoropyridines, and fluorinated oxygen containing alkyl side chains were investigated. Substituents at the oxime functionality are well tolerated and resulted in five candidates with K_i values below 10 nM. The most promising candidate, (*E*)-3-(pyridin-2-ylethynyl)cyclohex-2-enone-*O*-2-(2-fluoroethoxy)-ethyloxime (**38**, K_i = 3.8 nM), was radiolabeled with fluorine-18. Scatchard analysis of [^{18}F]**38** which modeled best for two sites pointed to high binding affinity (K_{D1} = 0.61 ± 0.19 nM and K_{D2} = 13.73 ± 4.69 nM) too. These data strongly suggest the further evaluation of [^{18}F]**38** as a candidate for imaging the mGluR5.

Introduction

The amino acid glutamate is the main excitatory neurotransmitter in the mammalian brain. Its transmission of neuronal signals is mediated by a large family of different glutamate receptors subdivided into two classes. On the one hand ionotropic glutamate receptors (i.e., kainate, α-amino-3-hydroxy-5-methyl-4-isoxazolepropionic acid (AMPA[a]), and *N*-methyl-D-aspartate (NMDA) receptors) mediate in general fast excitatory neurotransmission. On the other hand, the eight metabotropic glutamate receptor subtypes (mGluRs) discovered only from 1991 on modulate ionotropic glutamate receptor activity and are known to conduct neurotransmission in a fine-tuned way. The mGluRs belong to the family of G-protein-coupled receptors (GPCRs) and are subdivided into three groups according to their sequence homology, receptor pharmacology, and signal transduction pathways. Group I consists of mGluR1 and mGluR5 that are mainly located postsynaptically and activate phospholipase C via a G_q protein, while group II mGluRs (mGluR2 and mGluR3) and group III mGluRs (mGluR4, -6, -7, and -8) are located presynaptically and are coupled to a G_i protein.[1−3]

The metabotropic glutamate receptors have been implicated in numerous central nervous system (CNS) disorders. Especially, mGluR5 was shown in cell culture and in several animal models to play a certain role for the development of neurodegenerative diseases like Alzheimer's disease[4,5] and Parkinson's disease[6,7] or CNS disorders such as schizophrenia,[8,9] depression, anxiety,[10] neuropathic pain,[11,12] drug addiction,[13] and fragile X syndrome.[14] Although the underlying pathophysiological processes are not yet well-understood, it is generally agreed that mGluR5 is an important future drug target and could provide a diagnostic target as well.[15]

The mGluR5 consists of a large extracellular N-terminus sheltering the orthosteric glutamate binding site,[16] the seven transmembrane domains (TMs) typical for GPCRs and an intracellular C-terminus that interacts with the G-protein. The orthosteric binding site is highly conserved among glutamate receptors, hampering the development of subtype-specific ligands. Most of the effort is therefore spent on the development of allosteric modulators with their binding site located within the seven TMs of the receptor protein.[17] The allosteric antagonist binding site of mGluR5[18] was investigated intensively with 2-methyl-6-(phenylethynyl)pyridine (MPEP, Figure 1, **1**)[12,18] and 2-((3-methoxyphenyl)ethynyl)-6-methylpyridine (M-MPEP, Figure 1, **2**),[19,20] two prototype allosteric antagonists with high

*To whom correspondence should be addressed. Phone: +41 44 633 7463. Fax: +41 44 633 1367. E-mail: simon.ametamey@pharma.ethz.ch.

[a] Abbreviations: AMPA, α-amino-3-hydroxy-5-methyl-4-isoxazolepropionic acid; CDPPB, 3-cyano-*N*-(1,3-diphenyl-1*H*-pyrazol-5-yl)-benzamide; CNS, central nervous system; DMF, *N*,*N*-dimethylformamide; ESI, electrospray ionization; Et_2O, diethyl ether; Et_3N, triethylamine; EtOAc, ethyl acetate; F-MTEB, 3-fluoro-5-((2-methylthiazol-4-yl)ethynyl)benzonitrile; F-PEB, 3-fluoro-5-(pyridine-2-ylethynyl)benzonitrile; GPCR, G-protein-coupled receptor; HEPES, 4-(2-hydroxyethyl)-piperazine-1-ethanesulfonic acid sodium salt; HPLC, high performance liquid chromatography; M-MPEP, 2-((3-methoxyphenyl)ethynyl)-6-methylpyridine; HRMS, high resolution mass spectroscopy; LRMS, low resolution mass spectroscopy; MeCN, acetonitrile; mGluR5, metabotropic glutamate receptor subtype 5; MPEP, 2-methyl-6-(phenylethynyl)pyridine; NMDA, *N*-methyl-D-aspartate; PEG200, polyethylene glycol 200; PET: positron emission tomography; rt, room temperature; SAR, structure−activity relationship; TBAF, tetra-*n*-butylammonium fluoride; TBS, *tert*-butyldimethylsilane; THF, tetrahydrofuran; TM, transmembrane domain.

Published on Web 04/22/2010

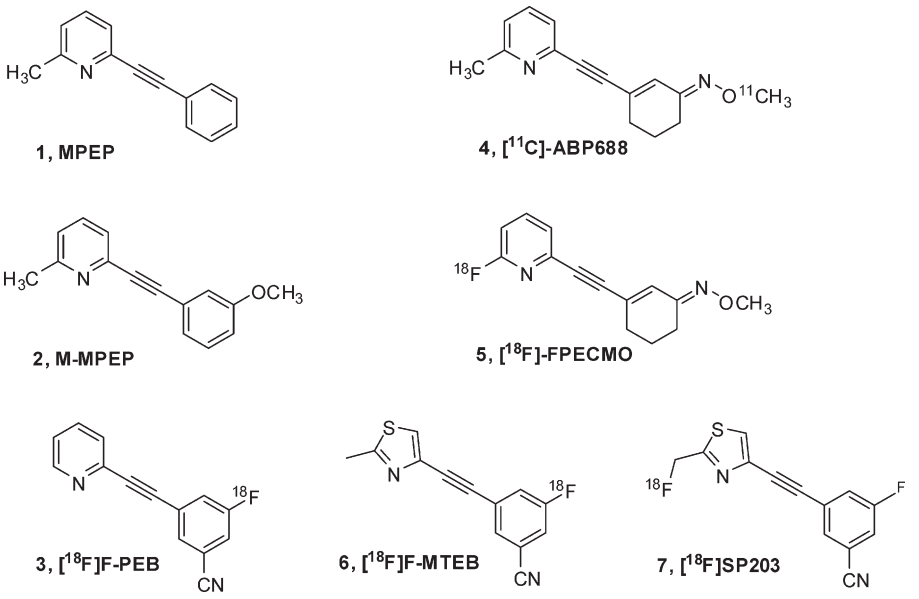

Figure 1. Structures of mGluR5 antagonists and radioligands.

Scheme 1. Synthetic Pathway toward Compounds with Varying Positions of the Nitrogen Atom in the Pyridine Ring (Series **1** Compounds)[a]

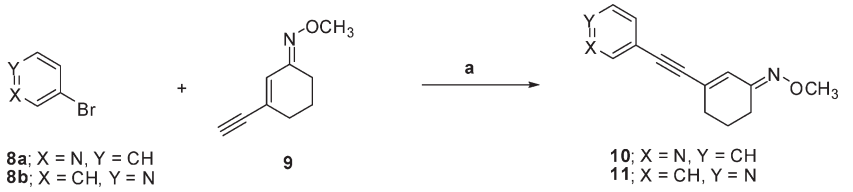

[a] Reagents and conditions: (a) $Pd(PPh_3)_4$, CuI, Et_3N, DMF, rt, 24 h.

binding affinity and selectivity for mGluR5. Important for MPEP binding to mGluR5 are residues in TMIII and TMVII on the one hand and TMV and TMVI on the other hand.[21] Binding to these TMs represents the general motif of many mGluR5 antagonists. Structurally, mGluR5 ligands such as MPEP and M-MPEP or radioligands like [^{18}F]3-fluoro-5-(pyridin-2-ylethynyl)benzonitrile[22] ([^{18}F]F-PEB, Figure 1, **3**), [^{18}F]3-fluoro-5-((2-methylthiazol-4-yl)ethynyl)benzonitrile[22] ([^{18}F]F-MTEB, Figure 1, **6**), and [^{18}F]-3-fluoro-5-(2-(2-(fluoromethyl)thiazol-4-yl)ethynyl)benzonitrile[23,24] ([^{18}F]SP203, Figure 1, **7**) consist of a heterocycle, most often a pyridine moiety that is connected via an acetylene linker to a second aromatic or heteroaromatic ring system. However, one of the most successful mGluR5 PET tracers and the first for imaging mGluR5 in humans, (*E*)-3-((6-methylpyridin-2-yl)ethynyl)-cyclohex-2-enone-*O*-[^{11}C]methyloxime ([^{11}C]ABP688, Figure 1, **4**),[25] slightly differs from this pattern. A cyclohexenoneoxime moiety (instead of a phenyl ring or a heteroaromatic ring system) is connected to a pyridine ring via the acetylene linker. Although **4** ([^{11}C]ABP688) is an excellent imaging agent, its use is limited to PET centers with a cyclotron and radiochemistry facilities mainly because of the short physical half-life of carbon-11. Consequently, there is a need for a fluorine-18 labeled analogue of **4** with similar imaging properties. The optimal physical half-life of fluorine-18 ($t_{1/2}$ = 110 min) permits the shipping of fluorine-18 labeled compounds over large distances and thus their commercial use.

The introduction of a fluorine atom into a molecule changes its structure and therefore affects properties such as lipophilicity, binding affinity, and chemical and metabolic stability. Recently, our group reported on [^{18}F](*E*)-3-((6-fluoropyridin-2-yl)ethynyl)cyclohex-2-enone-*O*-methyloxime[26] ([^{18}F]F-PEC-MO, Figure 1, **5**), the first fluorinated analogue of **4** bearing fluorine-18 at the pyridine functionality. Radiotracer **5** exhibits high in vitro binding affinity toward mGluR5 but shows rapid defluorination in vivo. In an effort to develop more stable fluorinated analogues, we designed and synthesized several new candidates that are amenable to fluorine-18 labeling by a one-step radiolabeling approach. Structure−activity relationship (SAR) studies were carried out to elucidate the optimal position of the fluorine atom. At first, the position of the nitrogen in the pyridine ring relative to the acetylene linker was shifted. In another approach, the methyl group at the oxime functionality in **4** was replaced by a variety of oxygen containing side chains, pyridines, and benzonitriles. Herein, we report on the syntheses and the binding affinities of these novel fluorinated analogues and present the fluorine-18 labeling of the most promising candidate.

Chemistry

In Scheme 1 is shown the synthetic pathway leading to compounds **10** and **11**. Alkyne derivative **9** was obtained as previously described.[26] Palladium catalyzed Sonogashira coupling[27] of **9** to 3-bromopyridine (**8a**) or 4-bromopyridine (**8b**) gave **10** or **11**, respectively, in reasonable yields. Compounds **16**−**18**, which are key intermediates for the preparation of a large series of **4** analogues, were prepared according to the reaction pathway outlined in Scheme 2. The reaction of ketone **12** with hydroxylamine hydrochloride yielded a mixture of

Scheme 2. Synthetic Pathway toward Key Intermediates **16**−**18**[a]

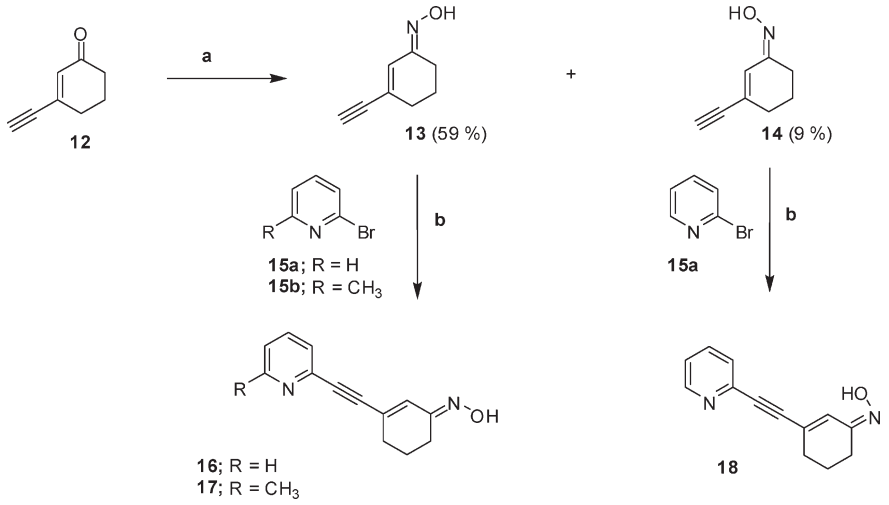

[a] Reagents and conditions: (a) $NH_2OH \cdot HCl$, pyridine, rt, 18 h; (b) $Pd(PPh_3)_4$, CuI, Et_3N, DMF, rt, 20 h.

Scheme 3. Synthetic Pathway toward Fluoropyridines (Series **2** Compounds) and Fluorobenzonitriles (Series **3** Compounds)[a]

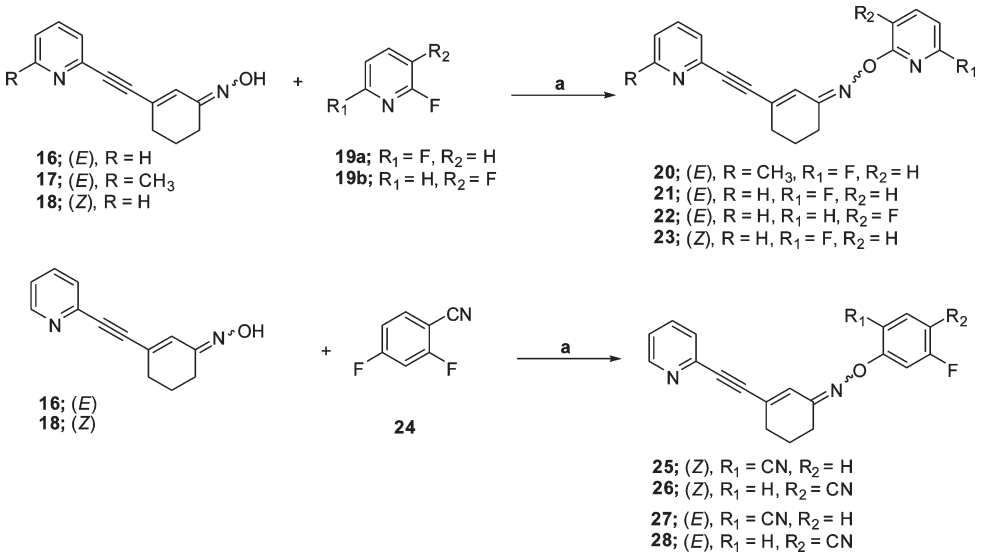

[a] Reagents and conditions: (a) DMF, NaH, rt, 2 h.

trans- and *cis*-oximes that were easily separated by flash column chromatography to give pure *trans*-**13** and *cis*-**14** in 59% and 9% yields, respectively. The Sonogashira coupling of the (*E*)-3-ethinylcyclohex-2-enoneoxime (**13**) with **15a** and **15b** gave key intermediates **16** and **17**, respectively, while the coupling of (*Z*)-3-ethinylcyclohex-2-enoneoxime (**14**) to **15a** afforded compound **18**.

Target compounds **20**−**23** were obtained by the reaction of 2,6-difluoropyridine (**19a**) with oximes **16**−**18** (Scheme 3). Synthon **16** was reacted with 2,3-difluoropyridine (**19b**) to give exclusively compound **22**. A third series of compounds containing fluorobenzonitriles at the oxime functionality of the **4** core structure is depicted in Scheme 3.

The synthesis of the compounds containing the cyano group was accomplished by reacting oximes **16** and **18** with 2,4-difluorobenzonitrile (**24**). Starting material **24** has potentially two positions for nucleophilic attack. Consequently, four products **25**−**28** were obtained from the two syntheses. Preferred was the substitution of the fluorine in para position to the cyano group. As a result, compound **26** obtained as a side product was not further characterized. Compound **25** could be used for further investigations. With oxime **16**, two products were obtained with **28** being the major product.

Series **4** compounds were obtained by the reaction of oxime **16** with oxygen containing aliphatic starting materials such as **29**, **30**, and **33**[28] as shown in Scheme 4. Compound **31** was synthesized by reacting **16** with 1-fluoroethanol (**29**) and dibromomethane in the presence of sodium hydride. The synthesis gave the desired end product **31** in moderate yields. Compound **32** was prepared in a similar way using 1-fluoropropanol (**30**) as starting material. For the synthesis of compound **38** (Scheme 4), an analogue with longer side chain, a slightly different approach was chosen starting from (2-(2-bromoethoxy)ethoxy)(*tert*-butyl)dimethylsilane (**33**)[28] which was prepared according to literature procedure. The addition of **33** to key intermediate **16** afforded **34** in good yield. Compound **34** was converted to the corresponding tosylate **36** after cleavage of the TBS group and reaction with tosyl chloride. Reaction of **36** with dry tetra-*n*-butylammonium fluoride (TBAF) resulted in the final product **38**. Since **38**

Scheme 4. Synthetic Pathway toward **4** Analogues with Oxygen Containing Side Chains (Series **4** Compounds)[a]

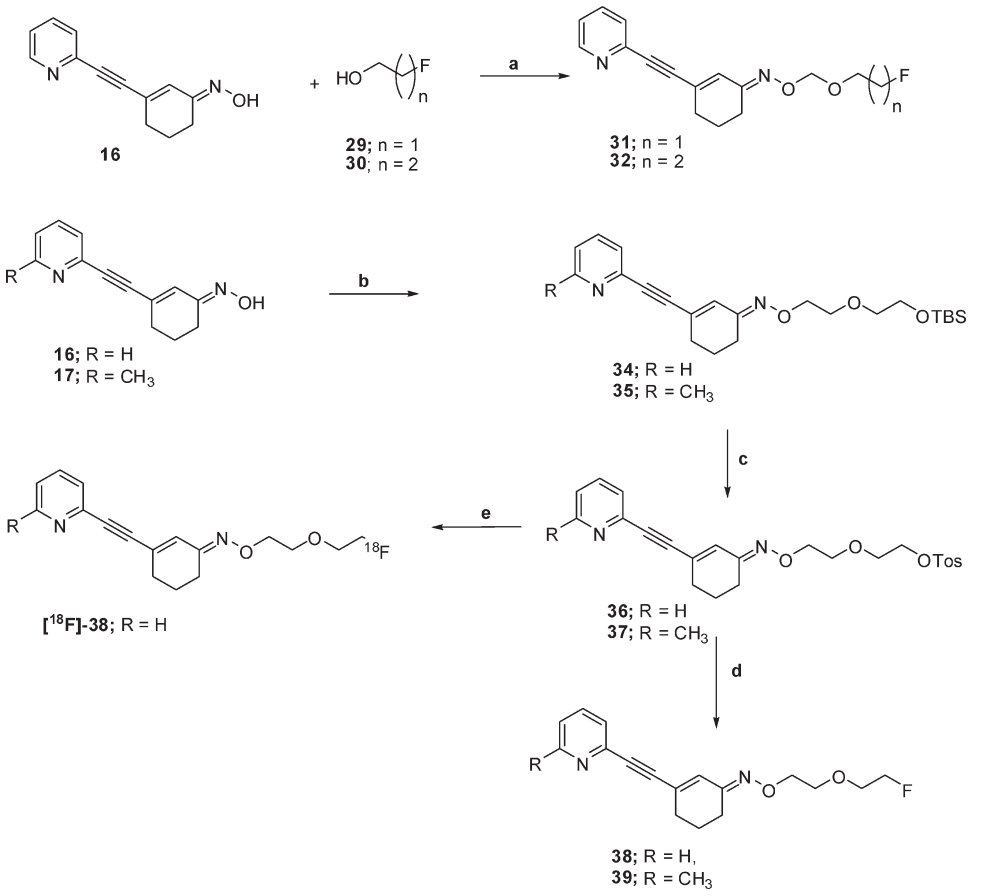

[a] Reagents and conditions: (a) DMF, NaH,CH_2Br_2, 40 min, rt; (b) (2-(2-bromoethoxy)ethoxy)(*tert*-butyl) dimethylsilane (**33**), DMF, NaH, 2 h, rt; (c) (1) THF, TBAF, 1.5 h, rt; (2) CH_2Cl_2, Et_3N, benzenesulfonyl chloride, 0 °C, 8 h; (d) TBAF, THF, 60 °C, 5 h; (e) K[^{18}F]F-Kryptofix 222, DMF, 90 °C, 10 min.

exhibited high binding affinity to mGluR5, compound **39** derived from key intermediate **17** was similarly synthesized for direct comparison (Scheme 4). For the one-step radiosynthesis of compound [^{18}F]**38**, tosylated synthon **36** served as the precursor.

Results and Discussion

Chemistry. The total syntheses of all target compounds were accomplished by convergent syntheses. The intermediates and products were obtained overall in satisfactory yields, although none of the synthesis steps was optimized. However, the formation of compounds **10** and **11** by Sonogashira coupling resulted in relatively low yields of 25 and 13%, respectively. In both cases purification by column chromatography over silica was problematic. Flash column chromatography finally turned out to be more efficient. The addition of dibromomethane to the sodium salts of compounds **16**, **29**, and **30** afforded compounds **31** and **32** in 31% and 18% yields, respectively. The low yields are probably due to competing reactions. But for our purposes, the yields are quite acceptable.

Structure−Activity Relationship Studies. Thirteen novel analogues of **4** were successfully synthesized and investigated for their binding affinity toward mGluR5. Competitive binding experiments were carried out with each candidate using [^{3}H]M-MPEP, a well characterized mGluR5 ligand, and employing rat brain membranes without cerebellum. Nonradioactive **4** was used for the determination of nonspecific binding. The resulting inhibition constants (K_i) of the compounds are listed in Table 1. The prototypical pyridine-3-yl and pyridine-4-yl analogues **10** and **11** with K_i values of 252 ± 25 and 54.8 ± 20.2 nM, respectively, were shown to be moderately potent binders with clearly reduced binding affinity compared to the lead compound **4** (K_i = 4.4 nM). The strategy to alter the position of the pyridine N-atom to stabilize analogues of **5** was thus not further pursued.

We next explored the possibility of incorporating substitutions at the oxime moiety of the core structure in order to investigate the tolerability of these substituents. An extensive survey of fluorine substituted pyridines and benzonitriles with several *trans*- and *cis*-oxime isomers of **4** was conducted. Also, derivatives of **4** lacking the methyl group in the pyridine ring were synthesized. The goal of improving or retaining nanomolar binding affinity was achieved for the series 2 compounds, in particular for compounds **21** (K_i = 9.15 ± 2.15 nM) and **22** (K_i = 4.01 ± 0.97 nM), which are both desmethyl analogues of **4**. From these series, the 3-fluoro substitution in the oxime-linked pyridine ring (R_2) exhibited the highest binding affinity. The corresponding methyl containing compound **20**, on the contrary, showed a 5-fold reduced affinity, which is ascribed to the presence of the methyl group on the acetylene-linked pyridine ring (R_1). However, other SAR studies showed that the presence of a methyl group in ortho position to the N-atom in heterocycles such as the pyridine ring (R_1) in **4** (Table 1) is well tolerated for mGluR5 binding or even improves mGluR5 binding.[30−32] Thus, we hypothesized that the reduction in binding affinity

Table 1. In Vitro Binding Data and clogP/log $D_{pH7.4}$ Values of Analogues of **4**[a]

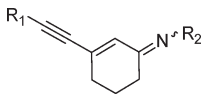

Compound number	R_1	R_2	K_i [nM][α]	clogP[δ] log$D_{pH7.4}$[ε]
10			**252 ± 25**	**1.9**
11			**54.8 ± 20.2**[β]	**1.9**
40[29]			**2.2**[γ]	**1.9**
4			**4.4**[γ]	**2.4** 2.4 ± 0.1[ε]
20		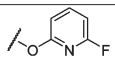	**46.8 ± 31.2**	**3.0**
21		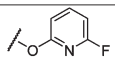	**9.15 ± 2.15**	**2.5**
22			**4.01 ± 0.97**[β]	**2.5**
23		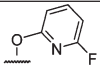	**44.04 ± 14.4**	**2.5**
25		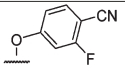	**49.80 ± 31.15**	**3.4**
28		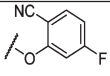	**73.38 ± 28.21**	**3.8**
27		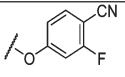	**56.10 ± 20.67**	**3.4**
31		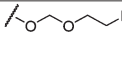	**8.41 ± 0.64**	**1.8**
32		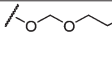	**5.42 ± 0.91**	**2.0**
38		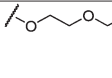	**3.8 ± 0.4**	**2.1** 1.7 ± 0.07[ε]
39		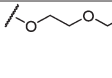	**26.8 ± 7.1**	**2.6** 2.1 ± 0.05[ε]

[a] The Greek symbols in the table have the following meaning: (α) K_i data obtained from three independent competition binding experiments in triplicate with the radioligand [^{3}H]M-MPEP and rat brain homogenate containing mGluR5; data are presented as the mean value followed by the standard deviation; (β) K_i data obtained from two independent competition binding experiments in triplicate; (γ) K_i data determined according to the standard procedure for competition binding experiments as a single determination in triplicate; (δ) calculated log *P* values (ChemDraw); (ε) experimentally obtained values ($n = 5$).

was related either to the overall size of the methylated analogue **20** or to the increased lipophilicity. Regarding the size, the two bulky moieties of **20** may exceed the size of the available space in the binding pocket. In terms of lipophilicity, the increase in K_i of the methylated ligand **20** would follow the general trend shown in Figure 3 whereby compounds with $K_i < 10$ nM have generally clogP values between 1.7 and 2.5, whereas compounds with $K_i \geq 10$ exhibited log *P* values greater than 2.5. Both hypotheses are in agreement with the K_i values of compounds **38** ($K_i = 3.8 \pm 0.4$ nM) and **39** ($K_i = 26.8 \pm 7.1$ nM). Also in this case, a 7-fold decreased affinity could be observed for the methyl containing derivative **39**.

The addition of relatively bulky R_2 groups, i.e., pyridines (compounds **20**−**23**) or benzonitriles (compounds **25**−**27**), including compounds with cis orientation (compounds **23** and **25**), affected the binding affinity of the derivatives of the lead compound **4** to a significantly lower extent than the shift of the nitrogen in compound **10**. Nonetheless, these compounds (**20**−**23**, **25**−**28**) did not show high enough binding affinity to be considered for further evaluation.

There were no significant differences in the binding affinities of the cis- and trans-isomers of the benzonitriles (compounds **25** and **27**, Table 1), again suggesting that the large size and/or the high lipophilicity of the benzonitrile moiety rather than structural features of the ligands reduced the binding affinity. In case of the smaller pyridine (R_2) analogues, K_i differed by a factor of 5 when cis- and trans-isomers **23** and **21** are compared. It is noteworthy that for compound **4** the trans-isomer is significantly a more potent binder than the cis-isomer.[25] The pegylated desmethyl analogues (**31**, **32**, and **38**) showed nanomolar binding affinities with the longer side chains exhibiting slightly higher affinities. The position of the oxygen in the side chain had only a marginal effect on the binding affinity.

The binding of MPEP and M-MPEP to mGluR5 involves TMIII, TMVII, TMV, and TMVI.[18] Whether **4** and our new ligands bind to exactly the same domains and whether they interact with similar amino acids or not remain unanswered. Nevertheless, the general structure of successful mGluR5 ligands, as described by Kulkarni et al.,[33] was retained for every novel candidate. Often, two aromatic moieties are connected via a convenient linker. This provides for interaction with two hydrophobic binding areas within the binding pocket of mGluR5. Keeping this concept led to the development of compound **38**. From all the analogues of **4** synthesized, compound **38** exhibited the highest binding affinity ($K_i = 3.8 \pm 0.4$ nM) to mGluR5 and was therefore selected for further evaluation as a PET tracer candidate.

Radiosynthesis and Saturation Binding Studies with [^{18}F]38. For the most promising candidate **38**, a radiosynthetic procedure for its [^{18}F]-labeled analogue, [^{18}F]-**38**, was successfully established (Scheme 4). The conversion of the tosylate precursor **36** into [^{18}F]**38** was accomplished using Kryptofix and K_2CO_3 as base in *N*,*N*-dimethylformamide (DMF). The reaction proceeded for 10 min at 90 °C and gave radiochemical yields between 25% and 35% (decay corrected). Semipreparative HPLC purification using acetonitrile (MeCN) and water as mobile phase resulted in high radiochemical purity (≥96%) of the final product. The specific activity of [^{18}F]**38** was in the range 110 − 350 GBq/μmol at the time of quality control.

The shake-flask method[34] was used to determine the log $D_{pH7.4}$ of [^{18}F]**38**. As expected from clogP calculations (Table 1), this ligand displays a moderate lipophilicity with a log *D* value of 1.7 ± 0.1 (Table 1, **38**). The measured log $D_{pH7.4}$ suggests that [^{18}F]**38** is sufficiently lipophilic for

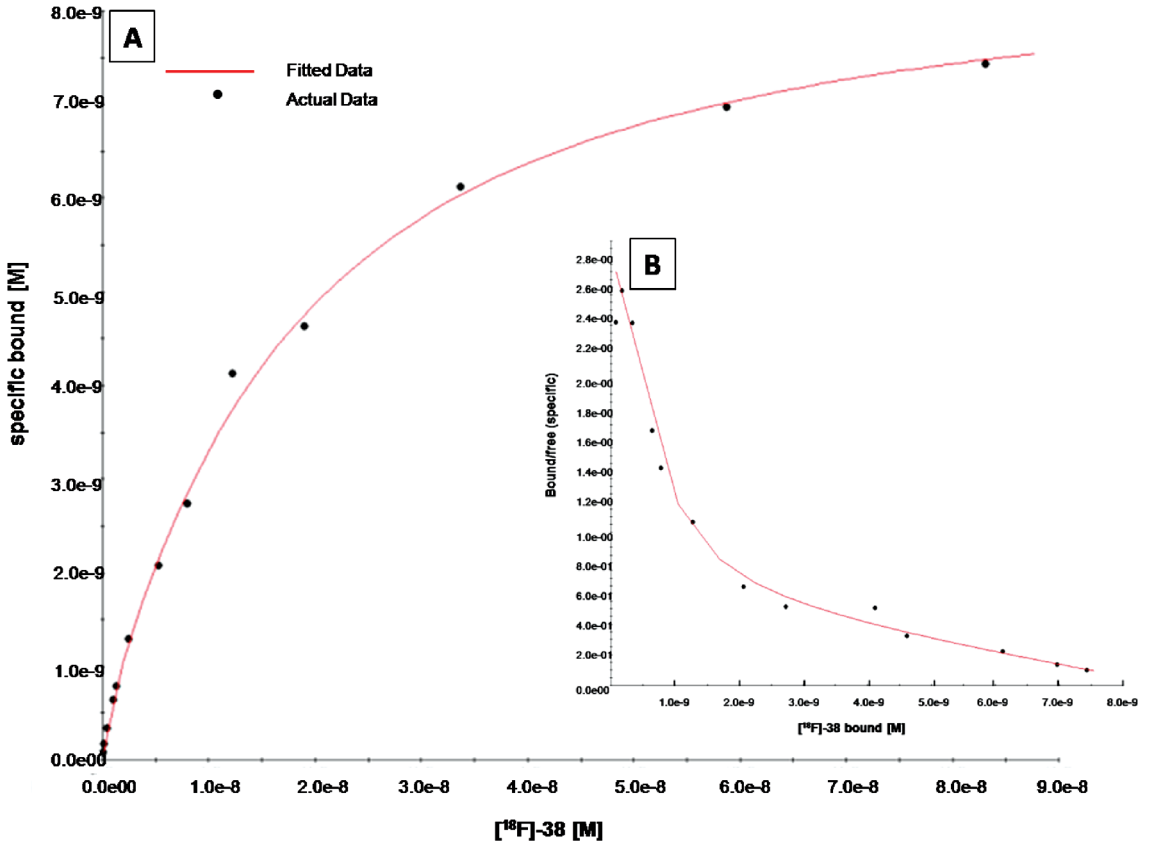

Figure 2. (A) Typical saturation binding curve of [^{18}F]**38** binding to rat brain membranes. (B) Representative Scatchard plot of [^{18}F]**38** saturation data. The dissociation constants obtained from three independent experiments are $K_{D1} = 0.6 \pm 0.2$ nM and $K_{D2} = 13.7 \pm 4.7$ nM.

free diffusion across the blood−brain barrier,[35] although this value is somewhat lower than the experimentally determined log *D* value of **4**. Efforts to increase the lipophilicity, however, resulted in reduced affinity as shown in Figure 3.

Further characterization of [^{18}F]**38** in a saturation binding assay with rat brain membranes revealed excellent binding affinity. A typical saturation curve and Scatchard plot analysis are shown in Figure 2. The Scatchard plots of three independent experiments were not linear as would be expected for one or more binding sites with equal binding affinity but were characterized by a steeper slope in the low concentration range than in the high concentration range. This was independent of whether total or specific binding was used for the analysis (data not shown). The binding data were fitted with a model assuming two different binding sites. The respective binding parameters for [^{18}F]**38** are $K_{D1} = 0.6 \pm 0.2$ and $K_{D2} = 13.7 \pm 4.7$ nM and B_{max1} and B_{max2} values ranging from 470 to 1870 fmol/mg and from 4.0 to 15.6 pmol/mg protein, respectively. On the basis of these data, we cannot conclude whether both binding sites are on mGluR5 or not. Note that the number of accessible binding sites is about 8 times higher for the site with the weaker binding affinity. The nonlinear Scatchard plots could alternatively indicate varying affinity states of one single binding site because of different receptor states, receptor−effector coupling, or decreasing receptor affinity caused by increasing receptor occupancy. Finally, artifacts due to technical problems are possible reasons for nonlinear Scatchard plots.[36]

So far, no mGluR5 antagonist sharing the same binding site as M-MPEP has been reported to bind to two distinct binding sites at the mGluR5. Only recently, Chen et al.[37,38] observed for a positive allosteric modulator of mGluR5,

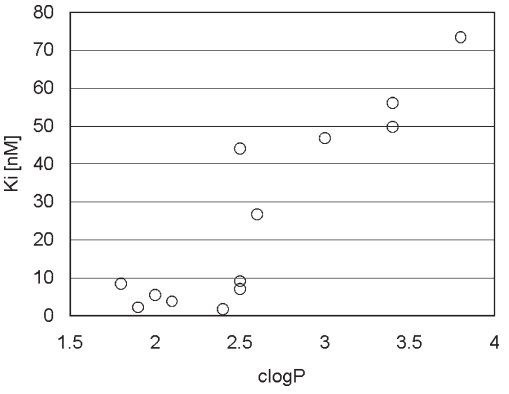

Figure 3. Correlation between inhibition constant (K_i) and clogP values of ligands **20**−**39**.

3-cyano-*N*-(1,3-diphenyl-1*H*-pyrazol-5-yl)benzamide (CDPPB),[39] binding to the binding site of negative allosteric modulators of mGluR5 such as MPEP in parallel. As Chen et al. hypothesize, CDPPB acts at overlapping binding sites in the transmembrane domain of mGluR5. However, the existence of multiple binding sites could lead to the results described above for compound **38**. Further studies are required to characterize the mGluR5 binding of **38** in more detail and to exclude high-affinity binding to other structures. Target specificity is indispensable for a successful PET tracer.

Conclusion

The synthesis and characterization of 13 novel analogues of **4** were successfully carried out. The binding affinities of the

compounds show that substituents at the oxime functionality are well tolerated. Five compounds exhibited K_i values below 10 nM. The most promising compound **38** was successfully labeled with fluorine-18 using a single-step radiosynthetic approach. The high binding affinity of [^{18}F]**38** to mGluR5 was confirmed by in vitro tests. Further in vitro evaluation and preclinical in vivo imaging with [^{18}F]**38** will show whether this tracer can even be used as a PET imaging agent for mGluR5 in humans.

Experimental Section

General Methods. Reagents and solvents utilized for experiments were obtained from commercial suppliers (Sigma-Aldrich, Alfa Aesar, Merck, and Fluka) and were used without further purification unless stated otherwise. [^{3}H]M-MPEP was provided by Novartis. Thin layer chromatography performed on precoated silica gel 60 F245 aluminum sheets suitable for UV absorption detection of compounds was used for monitoring reactions. Nuclear magnetic resonance spectra were recorded with a Bruker 400 MHz spectrometer with an internal standard from solvent signals. Chemical shifts are given in parts per million (ppm) relative to tetramethylsilane (0.00 ppm). Values of the coupling constant, *J*, are given in hertz (Hz). The following abbreviations are used for the description of ^{1}H NMR and ^{13}C NMR spectra: singlet (s), doublets (d), triplet (t), quartet (q), quintet (quint), doublet of doublets (dd), multiplet (m). The chemical shifts of complex multiplets are given as the range of their occurrence. Low resolution mass spectra (LRMS) were recorded with a Micromass Quattro micro API LC electrospray ionization (ESI). High resolution mass spectra (HRMS) were recorded with a Bruker FTMS 4.7 T BioAPEXII (ESI). Quality control of the final products in order to confirm the purity of ≥95% of the novel compounds was achieved by analytical high performance liquid chromatography (HPLC). It was performed on an Agilent 1100 system equipped with a radiodetector from Raytest using a reversed phase column (Gemini 10 μm C18, 300 mm × 3.9 mm, Phenomenex) by applying an isocratic solvent system with 70% MeCN in water and a flow of 1 mL/min.

Membrane Preparation. Competition binding assays for determination of mGluR5 binding affinity were carried out using rat brain membranes. For the preparation of these membranes male Sprague−Dawley rats were sacrificed by decapitation followed by quick removal of the brain including the olfactory bulb. After separation of the cerebellum the brain tissue was homogenized in 10 volumes of ice-cold sucrose buffer (0.32 M sucrose, 10 mM Tris/acetate buffer, pH 7.4) with a Polytron (PT-1200 C, Kinematica AG) for 1 min at setting 4. The obtained homogenate was centrifuged (1000*g*, 15 min, 4 °C) to give a pellet (P1). The supernatant was collected, and P1 was resuspended in 5 volumes of sucrose buffer. After homogenization and centrifugation, the supernatant was collected and combined with the supernatant before. Centrifugation of the obtained mixture (17000*g*, 20 min, 4 °C) resulted in a pellet (P2), which was resuspended with incubation buffer (5 mM Tris/acetate buffer, pH 7.4). The suspension was again centrifuged (17000*g*, 20 min, 4 °C) followed by resuspension of the resulting pellet with incubation buffer to obtain the final membrane preparation suitable for storage at −70 °C. For assays, the membranes were thawed and kept on ice during all of the preparation processes. The protein concentration was determined before each experiment by Bio-Rad microassay with bovine serum albumin as a standard (Bradford).[40]

Competition Binding Assays. P2 membranes were incubated with increasing concentrations of test compound (1 pM to 100 μM), each in triplicate, in incubation buffer II (30 mM 4-(2-hydroxyethyl)piperazine-1-ethanesulfonic acid sodium salt (HEPES), 110 mM NaCl, 5 mM KCl, 2.5 mM $CaCl_2 \cdot H_20$, 1.2 mM $MgCl_2$, pH 8). Radioligand [^{3}H]M-MPEP (2 nM) was added. Nonspecific binding was determined in the presence of unlabeled **4** (100 μM). Total binding of radioligand was obtained with only buffer and membranes. The test samples with a total volume of 200 μL were incubated for 45 min at room temperature (rt). In order to separate free radioligand from the membranes, 4 mL of ice-cold incubation buffer II was added followed by vacuum filtration over GF/C filters (Whatman). After rinsing the filters twice with 4 mL of buffer II, 4 mL of scintillation liquid (Ultima Gold, Perkin-Elmer) was added to the filters in β scintillation vials. With a β counter (Beckman Instruments, LS 6500, multipurpose scintillation counter) the radioactivity retained on the filters was measured. The data were evaluated with KELL Radlig software (Biosoft). For calculation of the K_i the Cheng−Prusoff equation is the underlying equation. Three independent experiments were performed for each end compound, except for compounds **11** and **22** ($n = 2$).

Saturation Assay. P2 membranes (500 μg/mL) were incubated with increasing concentrations of [^{18}F]**38** (0.25−100 nM) each in triplicate in ice-cold incubation buffer II to give a total volume of 200 μL. Nonspecific binding was determined in the presence of 100 μM unlabeled **4** for each concentration of [^{18}F]**38** in triplicate. The test samples were incubated for 45 min at rt before addition of 4 mL of ice-cold incubation buffer II, and vacuum filtration over GF/C filters (Whatman) pretreated with 0.05% PEI solution was performed. The filters were rinsed twice with 4 mL of incubation buffer II before each filter was prepared for measurement in an appropriate vial for measurement of the activity retained on the filter using a γ-counter (Wizard, Perkin-Elmer). Data analysis was performed for saturation and Scatchard analysis with Kell-Radlig computer program (McPherson & Biosoft, Cambridge, U.K., 1997). Three independent experiments were carried out with [^{18}F]**38** obtained from three independent radiosynthetical productions.

Determination of the Lipophilicity of [^{18}F]38 and of [^{18}F]39 (log $D_{pH7.4}$). Radiosynthesis of [^{18}F]**39** was performed in analogy to the radiolabeling for [^{18}F]**38** (see below). As described in Wilson et al.[34] for the shake flask method, 500 μL of octanol saturated with phosphate buffer (Soerensen, pH 7.4) and 500 μL of phosphate buffer saturated with octanol were pipetted into an Eppendorf cup. After addition of 10 μL of radiotracer solution the samples were shaken for 15 min. Centrifugation at 5000 rpm for 3 min was performed to separate the phases. Then 50 μL of each phase was pipetted into Eppendorf cups for measurement of the distribution of the activity with a γ-counter (Wizard, Perkin-Elmer). The experiment was performed in quintuplicate.

Radiosynthesis of [^{18}F]38. [^{18}F]Fluoride was produced via the ^{18}O(p,n)^{18}F reaction in a cyclotron using enriched ^{18}O-water. For trapping of $^{18}F^-$ from the aqueous solution it was passed through a light QMA cartridge (Waters) preconditioned with 0.5 M K_2CO_3 (5 mL) and water (5 mL). For elution of $^{18}F^-$ from the cartridge into a tightly closed 5 mL reaction vial, 1 mL of Kryptofix K_{222} solution (Kryptofix K_{222}; 2.5 mg of K_2CO_3, 0.5 mg in MeCN/water (3:1)) was used. The solvents were evaporated at 110 °C under vacuum in the presence of a slight in-flow of nitrogen gas. After addition of MeCN (1 mL), azeotropic drying was carried out as described above. The drying procedure was repeated twice. A solution of the corresponding precursor **36**, 2 mg in 300 μL of dry DMF, was then added to the kryptofix complex and the reaction mixture was heated at 90 °C for 10 min before 2 mL of MeCN in water (1:1) was added. Purification by semipreparative HPLC was carried out on a HPLC system equipped with a Merck-Hitachi L-6200A intelligent pump, a Knauer variable wavelength monitor UV detector, and a Geiger Müller LND 714 counter with Eberlein RM-14 instrument using a reversed phase column (Gemini 5 μm C18, 250 mm × 10 mm, Phenomenex) with a solvent system and gradient as follows: H_2O (solvent A), MeCN (solvent B); flow 5 mL/min; 0−10 min, 5% B; 10−20 min, 5% B → 50% B; 20−50 min, 50% B. The fraction containing the product was collected, and the mobile phase was evaporated under vacuum. The product was finally dissolved in PEG200/water (1:1). Determination of relative lipophilicity, radiochemical purity, and specific activity

was carried out during the quality control step. Identification of [^{18}F]**38** was achieved by coinjection with reference **38** to the HPLC system during quality control.

(*E*)-3-(Pyridin-2-ylethynyl)cyclohex-2-enoneoxime (16). A solution of 2-bromopyridine **15a** (2.444 g, 15.5 mmol) in DMF (12 mL) was carefully degassed and placed under argon atmosphere before $Pd(PPh_3)_4$ (110 mg, 0.097 mmol) was added. After the mixture was stirred for 5 min, Et_3N (6 mL) was added, and after further 5 min CuI (77 mg, 0.4 mmol) was added. A solution of **13** (2.013 g, 14.9 mmol) in DMF (20 mL) was prepared and poured into the reaction mixture. After stirring the mixture for 24 h at rt the synthesis was quenched with saturated NH_4Cl and extracted with EtOAc. The combined organic layers were washed with water and brine before evaporation under reduced pressure. Purification by column chromatography pentane/EtOAc (85:15 → 7:3) led to yellow crystals (2.7 g, yield = 85%). ^{1}H NMR (400 MHz, $CDCl_3$): δ 8.59 (d, J = 5.2 Hz, 1H), 7.67 (t, J = 7.8 Hz, 1H), 7.46 (d, J = 8.3 Hz, 1H), 7.23 (t, J = 6.2 Hz, 1H), 6.63 (s, 1H), 2.64 (t, J = 6.8 Hz, 2H), 2.41 (t, J = 6.8 Hz, 2H), 1.83 (quint, J = 6.8 Hz, 2H). ^{13}C NMR (100 MHz, $CDCl_3$): δ 20.8, 21.5, 29.2, 90.3, 91.5, 122.9, 127.0, 127.2, 131.8, 136.4, 143.1, 149.9, 156.2. MS m/z 212.95 $(M + H)^+$. HRMS calcd for $C_{13}H_{12}N_2O$, 212.0950; found 212.0945.

(*E*)-3-(Pyridin-2-ylethynyl)cyclohex-2-enone-*O*-2-(2-(*tert*-butyldimethylsilyloxy)ethoxy)ethyloxime (34). To a solution of *trans*-3[(pyridine-2-yl)ethynyl]cyclohex-2-enoneoxime **16** (151 mg, 0.71 mmol) in DMF (15 mL) was added 60% NaH (37 mg, 0.92 mmol). After the mixture was stirred for 30 min at rt, 2-(2-bromoethoxy)-(*tert*-butyl)dimethylsilane **33** (262 mg, 0.92 mmol) was added while the color changed quickly from yellow to light brown. After 1.5 h, 50% $NaHCO_3$ solution was added, and after a further 5 min the reaction mixture was extracted with ethyl acetate (3 × 20 mL). The combined organic layers were washed with water (2 × 20 mL) and brine and dried over Na_2SO_4 before the solvent was evaporated under reduced pressure. The obtained crude product was purified by column chromatography over silica using pentane/EtOAc (6:4), which gave a yellow oil (253 mg, yield = 86%). ^{1}H NMR (400 MHz, $CDCl_3$): δ 8.59 (d, J = 5.9 Hz, 1H), 7.65 (t, J = 7.4 Hz, 1H), 7.44 (d, J = 8.2 Hz, 1H), 7.22 (t, J = 6.4 Hz, 1H), 6.57 (s, 1H), 4.26 (t, J = 5.2 Hz, 2H), 3.76 (q, J = 5.1 Hz, 4H), 3.56 (t, J = 5.3 Hz, 2H), 2.58 (t, J = 6.8 Hz, 2H), 2.40 (t, J = 6.1 Hz, 2H), 1.80 (quint, J = 6.9 Hz, 2H), 0.90 (s, 9H), 0.07 (s, 6H). ^{13}C NMR (100 MHz, $CDCl_3$): δ −5.3, 18.4, 20.8, 22.3, 25.9, 29.4, 62.8, 69.8, 72.7, 73.8, 90.1, 91.6, 122.9, 127.1, 127.3, 131.2, 136.3, 143.1, 150.0, 155.6. MS m/z 415.09 $(M + H)^+$. HRMS calcd for $C_{23}H_{34}N_2NaO_3Si^+$, 437.2231; found, 437.2224.

(*E*)-3-((6-Methylpyridin-2-yl)ethynyl)cyclohex-2-enone-*O*-2-(2-(*tert*-butyldimethylsilyloxy)ethoxy)ethyloxime (35). This compound was prepared in an analogous way to **34**. Starting materials **17** (491 mg, 2.17 mmol) in DMF (40 mL) and **33** (550 mg, 1.94 mmol) gave the desired product (380 mg, yield = 45%). ^{1}H NMR (400 MHz, $CDCl_3$): δ 7.53 (t, J = 7.9 Hz, 1H), 7.27 (d, J = 7.4 Hz, 1H), 7.08 (d, J = 7.2 Hz, 1H), 6.56 (s, 1H), 4.25 (t, J = 5.5 Hz, 2H), 3.78−3.73 (m, 4H), 3.58 (t, J = 5.2 Hz, 2H), 2.58 − 2.55 (m, 5H), 2.38 (t, J = 7.1 Hz, 2H), 1.78 (quint, J = 6.8 Hz, 2H), 0.89 (s, 9H), 0.06 (s, 6H). ^{13}C NMR (100 MHz, $CDCl_3$): δ −5.2, 18.4, 20.8, 22.3, 26.0, 29.4, 62.8, 69.8, 72.7, 73.4, 73.8, 89.5, 92.9, 122.7, 124.5, 127.3, 131.0, 136.4, 142.7, 156.0, 159.2. MS m/z: 429.16 $(M + H)^+$.

(*E*)-2-(2-(3-(Pyridin-2-ylethynyl)cyclohex-2-enylideneaminooxy)-ethoxy)ethyl 4-Methylbenzenesulfonate (36). To a solution of **34** (230 mg, 0.55 mmol) in dry tetrahydrofuran (THF, 12.5 mL) was added 1 M TBAF (195 μL). After the mixture was stirred for for 1 h, water (10 mL) was added. The solution was extracted with EtOAc (3 × 20 mL), and the organic layers were washed with water (2 × 20 mL) and brine (30 mL) before drying over Na_2SO_4. The brown crude was obtained after evaporation of the solvent under reduced pressure. It was used without further purification. 3-[Pyridine-2-yl)ethynyl]cyclohex-2-enone-*O*-(2-oxyethyl)oxyethyloxime (crude, 85 mg) was dissolved in dry CH_2Cl_2 (2 mL). After addition of Et_3N (118 μL) the mixture was set to 0 °C. Finally, benzenesulfonyl chloride (114.39 mg, 0.6 mmol) was added, and after 8 h the mixture was diluted with water. Extraction with Et_2O (3 × 20 mL) and washing the organic layers with water (2 × 20 mL) and brine (30 mL) before drying over Na_2SO_4 led after evaporation to 176 mg of crude product. Purification by column chromatography using Et_2O/pentane (5:1) resulted in a yellow oil (67 mg, yield = 50%). ^{1}H NMR (400 MHz, $CDCl_3$): δ 8.59 (d, J = 5.2 Hz, 1H), 7.80 (d, J = 8.4 Hz, 2H), 7.65 (t, J = 8.0 Hz, 1H), 7.44 (d, J = 8.1 Hz, 1H), 7.33 (d, J = 8.3 Hz, 2H), 7.22 (t, J = 6.6 Hz, 1H), 6.56 (s, 1H), 4.17 (q, J = 4.2 Hz, 4H), 3.69 (q, J = 4.5 Hz, 4H), 2.55 (t, J = 7.1 Hz, 2H), 2.44 (s, 3H), 2.40 (t, J = 6.1 Hz, 2H), 1.80 (quint, J = 6.4 Hz, 2H). ^{13}C NMR (100 MHz, $CDCl_3$): δ 20.8, 21.7, 22.6, 29.4, 68.7, 69.2, 69.8, 77.2, 89.8, 91.9, 122.9, 127.3, 127.4, 128.0, 129.8, 130.9, 133.0, 136.2, 143.2, 144.8, 150.1, 155.8. MS m/z 455.01 (M+). HRMS calcd for $C_{24}H_{27}N_2O_5S^+$, 455.1635; found, 455.1631.

3-[Pyridine-2-yl)ethynyl]cyclohex-2-enone-*O*-fluoroethyloxy-ethyloxime (38). TBAF·$3H_2O$ (227 mg, 0.71 mmol) was dried on a high vacuum system at 45 °C for 24 h and was then dissolved in dry THF (5 mL). A solution of **36** (130 mg, 0.29 mmol) in dry THF (12 mL) was added, and after stirring the mixture for 5 h at 60 °C, water (10 mL) was added. The solution was extracted with Et_2O, and the organic layers were washed with water (2 × 20 mL) and brine (1 × 20 mL) before drying over Na_2SO_4. The brown crude, which was obtained after evaporation, was purified by column chromatography over silica with Et_2O/pentane (2:1) which afforded the desired product (49 mg, yield = 56%), 95% purity by HPLC (t_R = 4.98 min). ^{1}H NMR (400 MHz, $CDCl_3$): δ 8.59 (d, J = 5.0 Hz, 1H), 7.67 (t, J = 7.8 Hz, 1H), 7.44 (d, J = 8.1 Hz, 1H), 7.22 (t, J = 6.9 Hz, 1H), 6.57 (s, 1H), 4.63 (t, J = 4.2 Hz, 1H), 4.51 (t, J = 4.2 Hz, 1H), 4.28 (t, J = 5.1 Hz, 2H), 3.79 (m, 3H), 3.71 (t, J = 4.0 Hz, 1H), 2.58 (t, J = 6.4 Hz, 2H), 2.40 (t, J = 6.2 Hz, 2H), 1.80 (quint, J = 6.3 Hz, 2H). ^{13}C NMR (100 MHz, $CDCl_3$): δ 20.8, 22.3, 24.6, 70.2, 70.7 (d, J = 19.1 Hz), 73.4, 83.5 (d, J = 168.0 Hz), 90.2, 92.2, 123.2, 127.6, 127.7, 131.4, 136.5, 143.6, 150.5, 156.1. ^{19}F NMR (376 MHz, $CDCl_3$): δ −223.10 (m, J = 20.36 Hz). MS m/z 303.01 (M+). HRMS calcd for $C_{17}H_{20}FN_2O_2$, 303.1503; found, 303.1498.

Acknowledgment. We acknowledge the technical support of Claudia Keller, Mathias Nobst, Lukas Dialer, and Phoebe Lam. We thank Christophe Lucatelli and Stefanie-Dorothea Krämer for fruitful discussions.

Supporting Information Available: Synthesis procedures, NMR spectroscopic data, MS analytical data for intermediates **13**, **14**, **17**, **18**, and **34**−**37** and final compounds **10**, **11**, **20**−**28**, **31**, **32**, and **39**, and HPLC results for final compounds **10**, **11**, **20**−**28**, **31**, **32**, and **39**. This material is available free of charge via the Internet at http://pubs.acs.org.

References

(1) Kew, J. N. C.; Kemp, J. A. Ionotropic and metabotropic glutamate receptor structure and pharmacology. *Psychopharmacology* **2005**, *179*, 4–29. Erratum: *Psychopharmacology* **2005**, *182* (2), 320−320 .
(2) Conn, P. J.; Pin, J.-P. Pharmacology and functions of metabotropic glutamate receptors. *Annu. Rev. Pharmacol.* **1997**, *37* (1), 205–237.
(3) Ritzén, A.; Mathiesen, J. M.; Thomsen, C. Molecular pharmacology and therapeutic prospects of metabotropic glutamate receptor allosteric modulators. *Basic Clin. Pharmacol.* **2005**, *97* (4), 202–213.
(4) Bruno, V.; Ksiazek, I.; Battaglia, G.; Lukic, S.; Leonhardt, T.; Sauer, D.; Gasparini, F.; Kuhn, R.; Nicoletti, F.; Flor, P. J. Selective blockade of metabotropic glutamate receptor subtype 5 is neuroprotective. *Neuropharmacology* **2000**, *39* (12), 2223–2230.
(5) Wang, Q.; Walsh, D. M.; Rowan, M. J.; Selkoe, D. J.; Anwyl, R. Block of long-term potentiation by naturally secreted and synthetic amyloid {beta}-peptide in hippocampal slices is mediated via activation of the kinases c-Jun N-terminal kinase, cyclin-dependent kinase 5, and p38 mitogen-activated protein kinase as well as metabotropic glutamate receptor type 5. *J. Neurosci.* **2004**, *24* (13), 3370–3378.

(6) Rouse, S. T.; Marino, M. J.; Bradley, S. R.; Awad, H.; Wittmann, M.; Conn, P. J. Distribution and roles of metabotropic glutamate receptors in the basal ganglia motor circuit: implications for treatment of Parkinson's disease and related disorders. *Pharmacol. Ther.* **2000**, *88* (3), 427–435.

(7) Ossowska, K.; Konieczny, J.; Wardas, J.; Pietraszek, M.; Kuter, K.; Wolfarth, S.; Pilc, A. An influence of ligands of metabotropic glutamate receptor subtypes on parkinsonian-like symptoms and the striatopallidal pathway in rats. *Amino Acids* **2007**, *32* (2), 179–188.

(8) Ohnuma, T.; Augood, S. J.; Arai, H.; McKenna, P. J.; Emson, P. C. Expression of the human excitatory amino acid transporter 2 and metabotropic glutamate receptors 3 and 5 in the prefrontal cortex from normal individuals and patients with schizophrenia. *Mol. Brain Res.* **1998**, *56* (1−2), 207–217.

(9) Pietraszek, T.; Berghe, C. V. Defending against injection attacks through context-sensitive string evaluation. *Lect. Notes Comput. Sci.* **2006**, *3858*, 124–145.

(10) Pilc, A.; Klodzinska, A.; Branski, P.; Nowak, G.; Palucha, A.; Szewczyk, B.; Tatarczynska, E.; Chojnacka-Wójcik, E.; Wieronska, J. M. Multiple MPEP administrations evoke anxiolytic- and antidepressant-like effects in rats. *Neuropharmacology* **2002**, *43* (2), 181–187.

(11) Cosford, N. D. P.; Tehrani, L.; Roppe, J.; Schweiger, E.; Smith, N. D.; Anderson, J.; Bristow, L.; Brodkin, J.; Jiang, X. H.; McDonald, I.; Rao, S.; Washburn, M.; Varney, M. A. 3-[(2-Methyl-1,3-thiazol-4-yl)-ethynyl]-pyridine: a potent and highly selective metabotropic glutamate subtype 5 receptor antagonist with anxiolytic activity. *J. Med. Chem.* **2003**, *46* (2), 204–206.

(12) Gasparini, F.; Lingenhöhl, K.; Stoehr, N.; Flor, P. J.; Heinrich, M.; Vranesic, I.; Biollaz, M.; Allgeier, H.; Heckendorn, R.; Urwyler, S.; Varney, M. A.; Johnson, E. C.; Hess, S. D.; Rao, S. P.; Sacaan, A. I.; Santori, E. M.; Veliçelebi, G.; Kuhn, R. 2-Methyl-6-(phenylethynyl)-pyridine (MPEP), a potent, selective and systemically active mGlu5 receptor antagonist. *Neuropharmacology* **1999**, *38* (10), 1493–1503.

(13) Chiamulera, C.; Epping-Jordan, M. P.; Zocchi, A.; Marcon, C.; Cottiny, C.; Tacconi, S.; Corsi, M.; Orzi, F.; Conquet, F. O. Reinforcing and locomotor stimulant effects of cocaine are absent in mGluR5 null mutant mice. *Nat. Neurosci.* **2001**, *4* (9), 873–874.

(14) Todd, P. K.; Mack, K. J.; Malter, J. S. The fragile X mental retardation protein is required for type-I metabotropic glutamate receptor-dependent translation of PSD-95. *Proc. Natl. Acad. Sci. U.S.A.* **2003**, *100* (24), 14374–14378.

(15) Bordi, F.; Ugolini, A. Group I metabotropic glutamate receptors: implications for brain diseases. *Prog. Neurobiol.* **1999**, *59* (1), 55–79.

(16) Takahashi, K.; Tsuchida, K.; Tanabe, Y.; Masu, M.; Nakanishi, S. Role of the large extracellular domain of metabotropic glutamate receptors in agonist selectivity determination. *J. Biol. Chem.* **1993**, *268* (26), 19341–19345.

(17) Pin, J. P.; Acher, F. The metabotropic glutamate receptors: structure, activation mechanism and pharmacology. *Curr. Drug Targets: CNS Neurol. Disord.* **2002**, *1* (3), 297–317.

(18) Pagano, A.; Ruegg, D.; Litschig, S.; Stoehr, N.; Stierlin, C.; Heinrich, M.; Floersheim, P.; Prezeau, L.; Carroll, F.; Pin, J.-P.; Cambria, A.; Vranesic, I.; Flor, P. J.; Gasparini, F.; Kuhn, R. The non-competitive antagonists 2-methyl-6-(phenylethynyl)pyridine and 7-hydroxyiminocyclopropan[*b*]chromen-1a-carboxylic acid ethyl ester interact with overlapping binding pockets in the transmembrane region of group I metabotropic glutamate receptors. *J. Biol. Chem.* **2000**, *275* (43), 33750–33758.

(19) Alagille, D.; Baldwin, R. M.; Roth, B. L.; Wroblewski, J. T.; Grajkowska, E.; Tamagnan, G. D. Synthesis and receptor assay of aromatic-ethynyl-aromatic derivatives with potent mGluR5 antagonist activity. *Bioorg. Med. Chem.* **2005**, *13* (1), 197–209.

(20) Malherbe, P.; Kratochwil, N.; Mühlemann, A.; Zenner, M.-T.; Fischer, C.; Stahl, M.; Gerber, P. R.; Jaeschke, G.; Porter, R. H. P. Comparison of the binding pockets of two chemically unrelated allosteric antagonists of the mGlu5 receptor and identification of crucial residues involved in the inverse agonism of MPEP. *J. Neurochem.* **2006**, *98* (2), 601–615.

(21) Malherbe, P.; Kratochwil, N.; Zenner, M.-T.; Piussi, J.; Diener, C.; Kratzeisen, C.; Fischer, C.; Porter, R. H. P. Mutational analysis and molecular modeling of the binding pocket of the metabotropic glutamate 5 receptor negative modulator 2-methyl-6-(phenylethynyl)-pyridine. *Mol. Pharmacol.* **2003**, *64* (4), 823–832.

(22) Hamill, T. G.; Krause, S.; Ryan, C.; Bonnefous, C.; Govek, S.; Seiders, T. J.; Cosford, N. D. P.; Roppe, J.; Kamenecka, T.; Patel, S.; Gibson, R. E.; Sanabria, S.; Riffel, K.; Eng, W.; King, C.; Yang, X.; Green, M. D.; O'Malley, S. S.; Hargreaves, R.; Burns, H. D. Synthesis, characterization, and first successful monkey imaging studies of metabotropic glutamate receptor subtype 5 (mGluR5) PET radiotracers. *Synapse* **2005**, *56* (4), 205–216.

(23) Siméon, F. G.; Brown, A. K.; Zoghbi, S. S.; Patterson, V. M.; Innis, R. B.; Pike, V. W. Synthesis and simple ^{18}F-labeling of 3-fluoro-5-(2-(2-(fluoromethyl)thiazol-4-yl)ethynyl)benzonitrile as a high affinity radioligand for imaging monkey brain metabotropic glutamate subtype-5 receptors with positron emission tomography. *J. Med. Chem.* **2007**, *50* (14), 3256–3266.

(24) Ametamey, S. M.; Treyer, V.; Streffer, J.; Wyss, M. T.; Schmidt, M.; Blagoev, M.; Hintermann, S.; Auberson, Y.; Gasparini, F.; Fischer, U. C.; Buck, A. Human PET studies of metabotropic glutamate receptor subtype 5 with ^{11}C-ABP688. *J. Nucl. Med.* **2007**, *48* (2), 247–252.

(25) Ametamey, S. M.; Kessler, L. J.; Honer, M.; Wyss, M. T.; Buck, A.; Hintermann, S.; Auberson, Y. P.; Gasparini, F.; Schubiger, P. A. Radiosynthesis and preclinical evaluation of ^{11}C-ABP688 as a probe for imaging the metabotropic glutamate receptor subtype 5. *J. Nucl. Med.* **2006**, *47* (4), 698–705.

(26) Lucatelli, C.; Honer, M.; Salazar, J.-F.; Ross, T. L.; Schubiger, P. A.; Ametamey, S. M. Synthesis, radiolabeling, in vitro and in vivo evaluation of [^{18}F]-FPECMO as a positron emission tomography radioligand for imaging the metabotropic glutamate receptor subtype 5. *Nucl. Med. Biol.* **2009**, *36* (6), 613–622.

(27) Sonogashira, K.; Tohda, Y.; Hagihara, N. Convenient synthesis of acetylenes—catalytic substitutions of acetylenic hydrogen with bromoalkenes, iodoarenes, and bromopyridines. *Tetrahedron Lett.* **1975**, No. 50, 4467–4470.

(28) Yeo, W.-S.; Min, D.-H.; Hsieh, R. W.; Greene, G. L.; Mrksich, M. Label-free detection of protein−protein interactions on biochips13. *Angew. Chem., Int. Ed.* **2005**, *44* (34), 5480–5483.

(29) Cosford, N. D. P.; Mc Donald, I. A.; Bleicher, L. S.; Cube, R. V.; Schweiger, E. J.; Vernier, J.-M.; Hess, S. D.; Varney, M. A.; Mark, A.; Munoz, B. Preparation of Heterocyclic Compounds and Methods of Use Thereof. PCT Int. Appl. WO 0116121 (A1), 2001.

(30) Wendt, J. A.; Deeter, S. D.; Bove, S. E.; Knauer, C. S.; Brooker, R. M.; Augelli-Szafran, C. E.; Schwarz, R. D.; Kinsora, J. J.; Kilgore, K. S. Synthesis and SAR of 2-aryl pyrido[2,3-*d*]pyrimidines as potent mGlu5 receptor antagonists. *Bioorg. Med. Chem. Lett.* **2007**, *17* (19), 5396–5399.

(31) Bach, P.; Nilsson, K.; Wallberg, A.; Bauer, U.; Hammerland, L. G.; Peterson, A.; Svensson, T.; Österlund, K.; Karis, D.; Boije, M.; Wensbo, D. A new series of pyridinyl-alkynes as antagonists of the metabotropic glutamate receptor 5 (mGluR5). *Bioorg. Med. Chem. Lett.* **2006**, *16* (18), 4792–4795.

(32) Bonnefous, C.; Vernier, J. M.; Hutchinson, J. H.; Chung, J.; Reyes-Manalo, G.; Kamenecka, T. Dipyridyl amides: potent metabotropic glutamate subtype 5 (mGlu5) receptor antagonists. *Bioorg. Med. Chem. Lett.* **2005**, *15* (4), 1197–1200.

(33) Kulkarni, S. S.; Nightingale, B.; Dersch, C. M.; Rothman, R. B.; Newman, A. H. Design and synthesis of noncompetitive metabotropic glutamate receptor subtype 5 antagonists. *Bioorg. Med. Chem. Lett.* **2006**, *16* (13), 3371–3375.

(34) Wilson, A. A.; Jin, L.; Garcia, A.; DaSilva, J. N.; Houle, S. An admonition when measuring the lipophilicity of radiotracers using counting techniques. *Appl. Radiat. Isot.* **2001**, *54* (2), 203–208.

(35) Dischino, D. D.; Welch, M. J.; Kilbourn, M. R.; Raichle, M. E. Relationship between lipophilicity and brain extraction of C-11-labeled radiopharmaceuticals. *J. Nucl. Med.* **1983**, *24* (11), 1030–1038.

(36) Limbird, L. E. *Cell Surface Receptors: A Short Course on Theory and Methods*, 3rd ed.; Springer Science and Business Media: New York, 2005; p 219.

(37) Chen, Y.; Nong, Y.; Goudet, C.; Hemstapat, K.; de Paulis, T.; Pin, J.-P.; Conn, P. J. Interaction of novel positive allosteric modulators of metabotropic glutamate receptor 5 with the negative allosteric antagonist site is required for potentiation of receptor responses. *Mol. Pharmacol.* **2007**, *71* (5), 1389–1398.

(38) Kinney, G. G.; O'Brien, J. A.; Lemaire, W.; Burno, M.; Bickel, D. J.; Clements, M. K.; Chen, T.-B.; Wisnoski, D. D.; Lindsley, C. W.; Tiller, P. R.; Smith, S.; Jacobson, M. A.; Sur, C.; Duggan, M. E.; Pettibone, D. J.; Conn, P. J.; Williams, D. L., Jr. A novel selective positive allosteric modulator of metabotropic glutamate receptor subtype 5 has in vivo activity and antipsychotic-like effects in rat behavioral models. *J. Pharmacol. Exp. Ther.* **2005**, *313* (1), 199–206.

(39) Lindsley, C. W.; Wisnoski, D. D.; Leister, W. H.; O'Brien, J. A.; Lemaire, W.; Williams, D. L.; Burno, M.; Sur, C.; Kinney, G. G.; Pettibone, D. J.; Tiller, P. R.; Smith, S.; Duggan, M. E.; Hartman, G. D.; Conn, P. J.; Huff, J. R. Discovery of positive allosteric modulators for the metabotropic glutamate receptor subtype 5 from a series of *N*-(1,3-diphenyl-1*H*- pyrazol-5-yl)benzamides that potentiate receptor function in vivo. *J. Med. Chem.* **2004**, *47* (24), 5825–5828.

(40) Bradford, M. M. Rapid and sensitive method for quantitation of microgram quantities of protein utilizing principle of protein−dye binding. *Anal. Biochem.* **1976**, *72* (1−2), 248–254.